Modeling and Motion Control of Mobile Robot for Lattice Type Welding

Yang Bae Jeon*, Sang Bong Kim
Department of Mechanical Engineering, College, Pukyong National University, Korea
Soon Sil Park
Renault Samsung Motors Co., Ltd 185, Shinho-dong, Kangseo-gu, Pusan 618-722, Korea

This paper presents a motion control method and its simulation results of a mobile robot for a lattice type welding. Its dynamic equation and motion control methods for welding speed and seam tracking are described. The motion control is realized in the view of keeping constant welding speed and precise target line even though the robot is driven for following straight line or curve. The mobile robot is modeled based on Lagrange equation under nonholonomic constraints and the model is represented in state space form. The motion control of the mobile robot is separated into three driving motions of straight locomotion, turning locomotion and torch slider control. For the torch slider control, the proportional-integral-derivative (PID) control method is used. For the straight locomotion, a concept of decoupling method between input and output is adopted and for the turning locomotion, the turning speed is controlled according to the angular velocity value at each point of the corner with range of 90° constrained to the welding speed. The proposed control methods are proved through simulation results and these results have proved that the mobile robot has enough ability to apply the lattice type welding line.

Key Words: Mobile Robot, Motion Control, Nonholonomic Constraints, Decoupling Method

Nomenclature

b : Distance between driving wheel and symmetry axis
d : Distance from P_0 to mass center of mobile robot
D : Viscous friction
I_c : Inertia moment of mobile robot excluding driving wheels and rotors of motors on a vertical axis through intersection between symmetry axis and driving wheel axis.
I_m : Inertia moment of wheel and motor rotor on wheel diameter
I_w : Inertia moment of wheel and motor rotor on driving wheel axis
J : Inertia moment of rotor
K_{Dp} : Derivative gain for the mobile robot
K_{Ds} : Derivative gain for the torch slider
K_{Is} : Integral gain for the torch slider
K_{Pp} : Proportional gain for the mobile robot
K_{Ps} : Proportional gain for the torch slider
l_s : Maximum distance of the seam tracking sensor
l_{ts} : Maximum distance of the torch slider
m_c : Mass of mobile robot excluding masses for driving wheels and rotors of DC motors
m_w : Mass of driving wheel including rotor of motor
P_c : Mass center of the mobile robot with coordinates (x_c, y_c)
P_o : Geometric center with coordinates (x_o, y_o), that is the intersection between symmetry and the driving wheel axis

* Corresponding Author,
E-mail : neomicro@dreamwiz.com
TEL : +82-51-620-1606; **FAX** : +82-51-621-1411
Department of Mechanical Engineering, College, Pukyong National University, Korea (Manuscript **Received** May 15, 2001; **Revised** October 26, 2001)

r_p : Radius of pinion
r_w : Radius of driving wheel
v_{weld} : Welding speed
x_s : Distance of the seam tracking sensor
x_{ts} : Distance of the torch slider
x_{tss} : Distance of the end of torch
$X-Y$: World coordinate system
$x-y$: Coordinate system fixed on the mobile robot

Greeks:

θ_{sm} : Motor shaft angle
τ_p : Torque acting on the left and right wheel
τ_s : Torque acting on the torch slider

1. Introduction

Usually, in welding process of the shipbuilding industry, ship bottom is assembled of several egg box type of blocks in order to enhance intensity. The egg box is completed by welding processes of horizontal, vertical and lattice types. Since the welding process is very complicated, it mainly depends on worker's experience. To realize an automatic welding process, in the case of using a manipulator type of welding robot, we can not avoid from several problems such as finding a slowly start welding point, mobility, cost, miniaturization, and so on.

Nowadays, as a method for automatic welding, a mobile type of welding robot is employed for welding line of horizontal type (Kang, C. J. et al., 2000), but it can not weld the lattice type of welding line. Usually, the corner part in the lattice had been welded by worker's hand. Since the working space is very narrow, the welding workers need robots with lightly weight and small size. Thus, the conventional 6 degrees-of-freedom (DOF) robots are not appropriate for the lattice welding. Therefore, in order to realize more compactly automatic welding under complicate welding environment, an intelligent type of welding robot with small size and lightly weight is needed to be developed.

Wheeled mobile robots (WMR) constitute a class of mechanical systems characterized by kinematic constraints that are not integrable and can not be eliminated from the model equations (dAndrea-Novel et al., 1991, Fierro and Lewis, 1995, Yun and Yamamoto, 1993). Thus, the standard planning and control algorithms developed for usual robotic manipulators without constraints are no more applicable. The modeling issue of the WMR for the motion planning and control design is still a relevant question. Campion et al. analyzed the structural properties and classification of kinematic and dynamical models of the WMR to give a general and unifying presentation of the modeling issue of the WMR (dAndrea-Novel et al., 1991, Campion et al., 1996). They took into account the restriction to the robot mobility induced by the constraints, and partitioned 5 classed by introducing the concepts of degree of mobility and manipulation. Most of efforts related to the mobile robot control are concentrated on the mobile manipulator that typically consists of a mobile platform and a robotic manipulator mounted upon the platform (Kang, J. G. et al., 2000, Yamamoto and Yun, 1999). Thus, coordination of manipulator and locomotion is one of the main research topics of the mobile manipulators. The majority of the early works on the mobile manipulators focuses on the coordination of locomotion and manipulation by considering the manipulator and the platform as two independent entities (Chung and Hong, 1999, Chung and Velinsky, 1999, Yamamoto and Yun, 1994). Also, they do not take the interactions with the environment into account.

In the case of a mobile robot for welding purposes, there are very complex problems such that the motion control must be done in the view of keeping constant welding speed and precise target line even though the robot is driven for following straight line or corner. To obtain good welding bead, the welding speed must be kept constant or at least in a predefined limited range. Furthermore, the position of the mobile robot must be controlled to asymptotically converge because of a limited length of torch slider. In addition, a slider of the mobile robot carrying torch must be controlled for the end of torch to be

kept at the welding target line.

In this paper, the mobile robot is modeled based on Lagrange equation under nonholonomic constraints and the model is represented in the state space form. To solve the above problems, three types of control algorithms for the welding mobile robot are suggested: straight locomotion, seam tracking and turning locomotion controls. A concept of decoupling method between input and output is adopted for the straight locomotion. The PID control method is used for the torch slider control to seam tracking, and for the turning locomotion. The turning speed is controlled by the angular velocity value at each point of the corner with range of 90° constrained to the welding speed. Simulations have been done to verify the effectiveness of the proposed control systems.

2. Modeling for Mobile Robot

2.1 Kinematical constraint equations

In this section, we derive the motion and constraint equations of the mobile platform with a geometrical motion as shown in Fig. 1. To get the kinematical equations and to control the mobile robot by the proposed methods which will be stated in the following sections with the following assumptions.

i. Robot has two rotating wheels for body motion control.

ii. Two driving wheels are positioned on an axis passed through the vehicle geometric center.

iii. Two passive wheels(castors) are installed at the bottom of front and rear for balance of mobile platform.

iv. A torch slider is located at the center of mobile robot and is composed of rack and pinion gear.

v. A seam tracking sensor is located at the upper side of torch and a compensating sensor is attached at the rear side of body, where two sensors are made of linear potentiometers.

vi. A proximity sensor is installed for detection of corner rotation point and it is attached at the front side of the body.

vii. An electric magnet is set up at the bottom of robot's center in order to enhance driving force.

viii. The mobile platform can only move in the direction normal to the axis of the driving wheels.

ix. The velocity component at the point contacted with the ground in the plane of the wheel is zero.

x. Although tremendous friction force acts on the mobile platform, the two motors have enough power to move it.

xi. The mobile platform is moving on a horizontal plane.

xii. When the mobile platform is driven at the corner in the lattice space, it turns around one point.

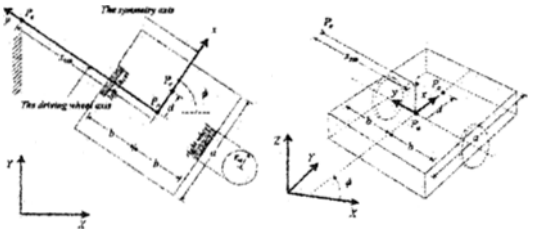

Fig. 1 Motion geometry of a mobile robot

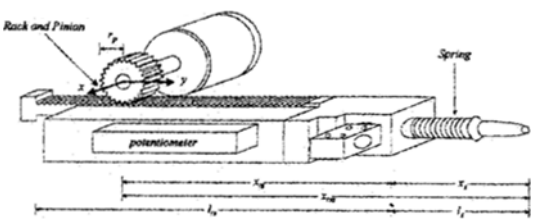

Fig. 2 Configuration of torch slider

The configuration of the torch slider can be described as shown in the Fig. 2.

If we ignore the passive wheels, the configuration of the mobile platform can be described by five generalized coordinates.

$$q=[x_c \ y_c \ \phi \ \theta_r \ \theta_l]^T \tag{1}$$

where ϕ is the heading angle of the mobile platform, and θ_r, θ_l are the angles of the right and left driving wheels, respectively. From assumptions

viii and ix, we can get the three constraints as follows. First, the velocity of the point P_c must be directed in the direction of the symmetry axis. The relation of velocity around P_c can be expressed as follows :

$$\dot{y}_c \cos\phi - \dot{x}_c \sin\phi - \dot{\phi} d = 0 \tag{2}$$

The other two constraints are obtained by the equations related to the velocities as follows :

$$\dot{x}_c \cos\phi + \dot{y}_c \sin\phi + b\dot{\phi} = r_w \dot{\theta}_r \tag{3}$$
$$\dot{x}_c \cos\phi + \dot{y}_c \sin\phi - b\dot{\phi} = r_w \dot{\theta}_l \tag{4}$$

Rearranging the above stated three constraints can be written in the form of

$$A(q)\,\dot{q} = 0 \tag{5}$$

where

$$A(q) = \begin{bmatrix} -\sin\phi & \cos\phi & -d & 0 & 0 \\ -\cos\phi & -\sin\phi & -b & r_w & 0 \\ -\cos\phi & -\sin\phi & b & 0 & r_w \end{bmatrix}$$

It is easy to check that $A(q)$ has rank 3. Consequently, the mobile platform has two DOF.

2.2 Dynamic equations of motion

The potential energy is zero ($V=0$) since it is assumed that the mobile platform is moving on a horizontal plane. The friction energy can be regarded as zero ($F=0$) from assumptions. Thus, the total kinetic energy T of the mobile robot is given by

$$T = \frac{1}{2} m(\dot{x}_c^2 + \dot{y}_c^2) + m_w d\dot{\phi}(\dot{x}_c \sin\phi - \dot{y}_c \cos\phi) + \frac{1}{2} I_w(\dot{\theta}_r^2 + \dot{\theta}_l^2) + \frac{1}{2} I\dot{\phi}^2 \tag{6}$$

where

$$m = m_c + 2m_w$$
$$I = I_c + 2m_w(b^2 + d^2) + 2I_m$$

To derive the dynamic equation for the mobile robot, we apply the well known Lagrange equation for nonholonomic constraints to the motion of the mobile platform as follows :

$$\frac{d}{dt}\left(\frac{\partial T}{\partial \dot{q}_i}\right) - \frac{\partial T}{\partial q_i} = \tau_i - \sum_{j=1}^{3} A^T_{ij}\lambda_i, \quad i = 1, \cdots, 5 \tag{7}$$

$$m\ddot{x}_c + m_w d(\ddot{\phi}\sin\phi + \dot{\phi}^2\cos\phi) = \lambda_1 \sin\phi + (\lambda_2 + \lambda_3)\cos\phi \tag{8}$$

$$m\ddot{y}_c - m_w d(\ddot{\phi}\cos\phi - \dot{\phi}^2\sin\phi) = \lambda_1 \cos\phi + (\lambda_2 + \lambda_3)\sin\phi \tag{9}$$

$$m_w d(\ddot{x}_c \sin\phi - \ddot{y}_c \cos\phi) + I\ddot{\phi} = d\lambda_1 - b(\lambda_3 - \lambda_2) \tag{10}$$

$$I_w \ddot{\theta}_r = \tau_r - \lambda_2 r_w \tag{11}$$

$$I_w \ddot{\theta}_l = \tau_l - \lambda_3 r_w \tag{12}$$

where λ_1, λ_2, λ_3 are Lagrange multipliers corresponding to 3 independent kinematical constraints. τ_r, τ_l are the torques acting on the right and left wheels, respectively. These five equations describing the motion of the mobile robot can easily be written by the following vector form.

$$M(q)\,\ddot{q} + V(q, \dot{q}) = E(q)\,\tau_p - A^T(q)\,\lambda \tag{13}$$

where

$$M(q) = \begin{bmatrix} m & 0 & m_w d\sin\phi & 0 & 0 \\ 0 & m & -m_w d\cos\phi & 0 & 0 \\ m_w d\sin\phi & -m_w d\cos\phi & I & 0 & 0 \\ 0 & 0 & 0 & I_w & 0 \\ 0 & 0 & 0 & 0 & I_w \end{bmatrix}$$

$$V(q, \dot{q}) = \begin{bmatrix} m_w d\dot{\phi}^2\cos\phi \\ m_w d\dot{\phi}^2\sin\phi \\ 0 \\ 0 \\ 0 \end{bmatrix}, \quad E(q) = \begin{bmatrix} 0 & 0 \\ 0 & 0 \\ 0 & 0 \\ 1 & 0 \\ 0 & 1 \end{bmatrix}, \quad \tau_p = \begin{bmatrix} \tau_r \\ \tau_l \end{bmatrix}$$

2.3 State space representation

To transform the above dynamic equation into the state space form, let us define that $S(q)$ is the null space of $A(q)$ so as to remove Lagrange multipliers. $S(q)$ is given by

$$S(q) = [s_1(q),\ s_2(q)] \tag{14}$$
$$= \begin{bmatrix} c(b\cos\phi - d\sin\phi) & c(b\cos\phi + d\sin\phi) \\ c(b\sin\phi + d\cos\phi) & c(b\sin\phi - d\cos\phi) \\ c & -c \\ 1 & 0 \\ 0 & 1 \end{bmatrix}$$

$$c = \frac{r_w}{2b}.$$

As the constraint Eq. (5) is zero, we can see that $\dot{q}$ is in the null space of $A(q)$. It follows that $\dot{q} \in span\{s_1(q),\ s_2(q)\}$, and it is possible to express $\dot{q}$ as a linear combination of $s_1(q)$ and $s_2(q)$, i.e.,

$$\dot{q} = s_1(q)\,\eta_1 + s_2(q)\,\eta_2 = S(q)\,\eta \tag{15}$$

and

$$\ddot{q}=S(q)\,\dot{\eta}+\dot{S}(q)\,\eta \tag{16}$$

For the specific choice of the matrix $S(q)$ in Eq. (14), we have $\eta=\dot{\theta}$, where $\dot{\theta}=[\dot{\theta}_r\ \dot{\theta}_l]^T$. Now, let us multiply $S^T(q)$ to both sides of the dynamic Eq. (13), then, we have

$$\begin{aligned} &S^T(q)\,M(q)\,\ddot{q}+S^T(q)\,V(q,\dot{q})\\ &=S^T(q)\,E(q)\,\tau_p-S^T(q)\,A^T(q)\,\lambda \end{aligned} \tag{17}$$

Using $S^T(q)\,A^T(q)=0$ and $S^T(q)\,E(q)=I_{2\times 2}$, and substituting the Eq. (16) for the above equation, we can obtain

$$\begin{aligned} &S^T(q)\,M(q)\,(S(q)\,\dot{\eta}+\dot{S}(q)\,\eta)\\ &+S^T(q)\,V(q,\dot{q})=\tau_p \end{aligned} \tag{18}$$

Using the state space variables, $x=[x_c\ y_c\ \phi\ \theta_r\ \theta_l\ \dot{\theta}_r\ \dot{\theta}_l]^T$, the dynamics of the mobile platform can be represented in the state space form :

$$\dot{x}=\begin{bmatrix} S\eta \\ -(S^TMS)^{-1}(S^TM\dot{S}\eta+S^TV) \end{bmatrix}+\begin{bmatrix} 0 \\ (S^TMS)^{-1} \end{bmatrix}\tau_p \tag{19}$$

To control the welding speed, first we must get the welding speed. In Fig. 3, when the mobile robot moves from $(i-1)$th position to (i)th position, the welding speed is calculated as follows :

$$\begin{aligned} v_{weld}&=\frac{d\overline{P_aP_e}}{dt}+v_c\sin\phi \\ &=\dot{x}_{tss}\cos\phi-x_{tss}\dot{\phi}\sin\phi+v_c\sin\phi=v(q) \end{aligned} \tag{20}$$

where

$$\overline{P_aP_e}=x_{tss}\sin(90-\phi),$$

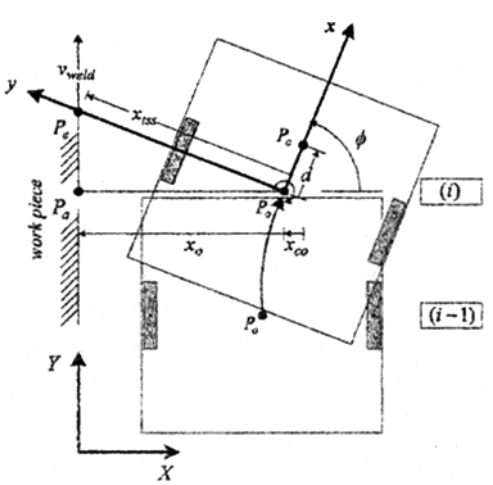

Fig. 3 Motion of the mobile platform

$$\frac{d\overline{P_aP_e}}{dt}=\dot{x}_{tss}\cos\phi-x_{tss}\dot{\phi}\sin\phi$$

where v_c is the forward velocity of the mobile robot. In Fig. 2, by appling the Newton's Second Law to the rotor, we can get the following equation.

$$J\frac{d^2\theta_{sm}}{dt^2}+D\frac{d\theta_{sm}}{dt}=\tau_s \tag{21}$$

Now, let us multiply radius of pinion at both sides of above equation and substitute $\ddot{x}_{ts}$ for $r_p\frac{d^2\theta_{sm}}{dt^2}$ and $\dot{x}_{ts}$ for $r_p\frac{d\theta_{sm}}{dt}$ because $r_p\theta_{sm}$ is the length of torch slider(x_{ts}). Then, we have

$$\ddot{x}_{ts}=-D_m\dot{x}_{ts}+C_m\tau_s \tag{22}$$

where

$$D_m=\frac{D}{J},\ C_m=\frac{r_p}{J}$$

The distance of the seam tracking sensor, x_s shown in Fig. 2, can be calculated by

$$x_s=\begin{cases} \dfrac{x_o}{\sin\phi}-x_{ts}=l(x_o,\,x_{ts},\,\phi) & :\ 0\le x_s\le l_s, \\ l_s & :\ x_s>l_s \end{cases} \tag{23}$$

The seam tracking sensor has a spring for making initial distance of the seam tracking sensor. Thus, if the value x_s is less than the maximum length, then, x_s can be calculated by Eq. (23). While x_s is lager than maximum length, x_s is set by the maximum length (l_s).

Now, by including the four state variables x_{ts}, $\dot{x}_{ts}$, $\dot{x}_s$, v_{weld} into Eq. (19), we can obtain the augmented state equation with all states for the mobile platform and torch slider as follows :

$$\dot{x}=\begin{bmatrix} S\eta \\ -(S^TMS)^{-1}(S^TM\dot{S}\eta+S^TV) \\ x_9 \\ -D_mx_9 \\ \dot{l}(x_0,\,x_8,\,x_3) \\ \dot{v}(q) \end{bmatrix}+\begin{bmatrix} 0 & 0 \\ -(S^TMS)^{-1} & 0 \\ 0 & 0 \\ 0 & C_m \\ 0 & 0 \\ 0 & 0 \end{bmatrix}\tau \tag{24}$$

where

$$\begin{aligned} x&=[x_1\ x_2\ x_3\ x_4\ x_5\ x_6\ x_7\ x_8\ x_9\ x_{10}\ x_{11}]^T\\ &=[x_c\ y_c\ \phi\ \theta_r\ \theta_l\ \dot{\theta}_r\ \dot{\theta}_l\ x_{ts}\ \dot{x}_{ts}\ x_s\ v_{weld}]^T,\\ \tau&=[\tau_r\ \tau_l\ \tau_s]^T. \end{aligned}$$

Then, the DOF of the mobile robot is three

because of added freedom of the torch slider. For the number of actuator inputs is equal to the DOF of the mobile robot, we can apply the following nonlinear feedback control for the mobile platform:

$$\tau_p=(S^TM\dot{S}\eta+S^TV)+(S^TMS)\,S^TEu_p \quad (25)$$

$$\tau_s=u_s \quad (26)$$

Let us define the control input as follows :

$$u=\begin{bmatrix}u_p\\u_s\end{bmatrix} \quad (27)$$

where u_p is the control input for the mobile platform and u_s is the control input for the slider. Then, the state equation can be simplified to the form :

$$\dot{x}=f(x)+g(x)\,u \quad (28)$$

where

$$f(x)=\begin{bmatrix}S\eta\\0\\x_9\\-D_mx_9\\\dot{l}(x_o,\,x_8,\,x_3)\\\dot{v}(q)\end{bmatrix}\quad g(x)=\begin{bmatrix}0&0\\I_{2\times2}&0\\0&0\\0&C_m\\0&0\\0&0\end{bmatrix}.$$

3. Control Algorithms

3.1 Torch slider control

To control the torch slider for seam tracking, a PID controller method is used. We may choose the following output equation :

$$y_s=h_s(x)=x_s \quad (29)$$

The tracking error for the seam tracking sensor is defined as follows :

$$e_s=x_s^d-x_s \quad (30)$$

The control input for the torch slider in Eq. (28) is designed by using the PID controller :

$$u_s=K_{Ps}e_s+K_{Is}\int e_s dt+K_{Ds}\dot{e}_s \quad (31)$$

3.2 Straight locomotion control

To control the welding speed, we control the velocity of the mobile platform. As the mobile platform has two motors, we may choose two output variables to control position and velocity of the robot shown in the output equation :

$$y_p=h_p(x)=[h_{p1}(q)\;\;h_{p2}(\eta)]^T=[y_{p1}\;\;y_{p2}]^T \quad (32)$$

where $h_{p1}(q)$ is defined as the shortest distance from point P_c of mass center to the desired path, and $h_{p2}(\eta)$ is the forward velocity of the mobile platform. To consider a straight line path, let the path be described by $Px+Qy+R=0$. Thus, we can derive the shortest distance, $h_{p1}(q)$ for the above path

$$h_{p1}(q)=h_{p1}(x_c,\,y_c)=\frac{Px_c+Qy_c+R}{\sqrt{P^2+Q^2}} \quad (33)$$

and the forward velocity of the mobile platform is given by

$$h_{p2}(\eta)=\dot{x}_c\cos\phi+\dot{y}_c\sin\phi=\frac{r_w}{2}(\eta_1+\eta_2) \quad (34)$$

The decoupling matrix for this output equation is computed as follows (Sarkar et al., 1994, Shankar, 1999) :

$$\dot{y}_{p1}=\frac{\partial h_{p1}}{\partial x}=J_{hp1}(q)\,S(q)\,\eta \quad (35)$$

$$\ddot{y}_{p1}=\frac{\partial[J_{hp1}(q)\,S(q)]}{\partial q}\eta+J_{hp1}(q)\,S(q)\,u_p \quad (36)$$

where

$$J_{hp1}(q)=\frac{\partial h_{p1}}{\partial q}=\frac{1}{\sqrt{P^2+Q^2}}[P\;Q\;0\;0\;0] \quad (37)$$

The output equation for forward velocity of the mobile platform can be given by

$$\dot{y}_{p2}=\frac{\partial h_{p2}}{\partial q}\dot{x}=J_{hp2}(q)\,u_p \quad (38)$$

where

$$J_{hp2}=\frac{\partial h_{p2}}{\partial q}=\begin{bmatrix}\frac{r_w}{2}&\frac{r_w}{2}\end{bmatrix} \quad (39)$$

Therefore, the decoupling matrix is yielded as

$$\Phi=\begin{bmatrix}J_{hp1}(q)\,S(q)\\J_{hp2}\end{bmatrix} \quad (40)$$

Because Φ is bounded away from zero for all x, we can derive the control input for the straight locomotion in Eq. (28) as follows :

$$u_p=\Phi^{-1}(v_p-\dot{\Phi}\eta) \quad (41)$$

where

$$v_p=\begin{bmatrix}v_1\\v_2\end{bmatrix}=\begin{bmatrix}K_{Pp}e_p+K_{Dp}e_p\\e_v\end{bmatrix}$$

Then, the path errors and forward velocity of the mobile robot are defined as follows :

$$\begin{bmatrix} e_p \\ e_v \end{bmatrix} = \begin{bmatrix} v_1^d - y_{p1} \\ v_2^d - y_{p2} \end{bmatrix}. \tag{42}$$

Table 1 Numerical values of the mobile robot

Parameters	Values	Units	Parameters	Values	Units
b	0.1045	m	m_c	16.9	kg
a	0.105	m	m_w	0.3	kg
d	0.01	m	I_c	0.2801	kgm^2
r_w	0.025	m	I_m	3.75e-4	kgm^2
r_p	0.02	m	I_w	4.96e-4	kgm^2
l_{ts}	0.3	m	J	100	Nm/s^2
l_s	0.1	m	D	0.01	

3.3 Turning locomotion control

A proximity sensor detects the rotation point at the corner, then, the robot rotates the corner for welding and its sliding arm is controlled for the end of torch to be kept at the welding target line. When the robot is driven at the corner in the lattice space, the left and right wheels are driven in the opposite direction. The absolute speed of two wheels is exactly equal. In addition, the electric magnet prevents to stray away from turn-

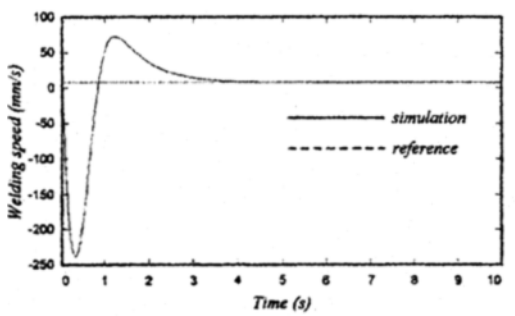

(a) The welding speed v_{weld}

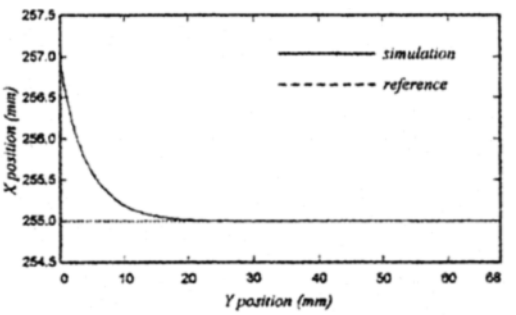

(b) The position x_c

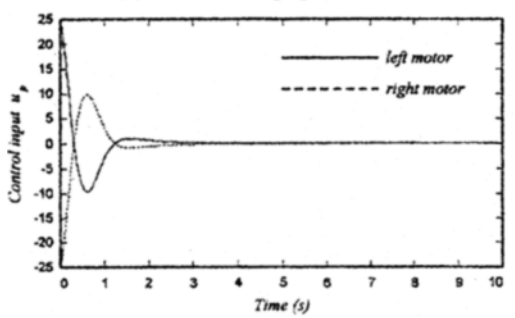

(c) Control input for mobile robot u_p

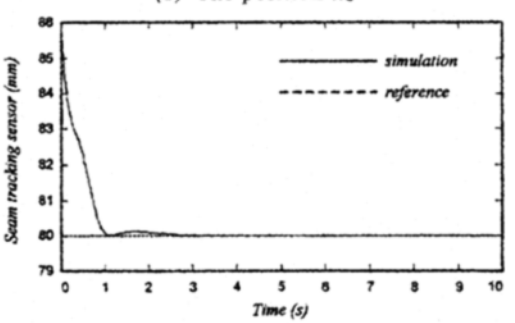

(d) Distance of the seam tracking sensor x_s

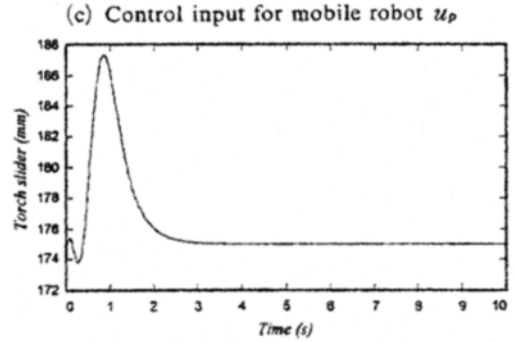

(e) Distance of the torch slider x_{ts}

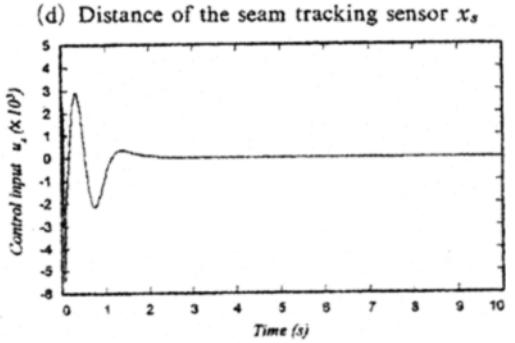

(f) Control input for torch slider u_s

Fig. 5 Simulation results of straight locomotion

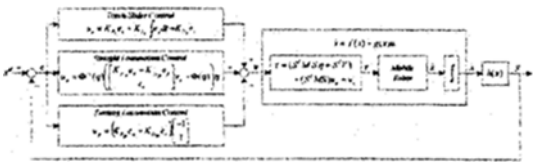

Fig. 4 Block diagram of the closed loop system

ing point. Thus, we already assumed that the forward velocity of the mobile platform is zero. By using Eq. (20) and the assumption, we can derive the welding speed as follows :

$$v_{weld}=\overline{P_aP_e'}=\dot{x}_{tss}\cos\phi-x_{tss}\dot{\phi}\sin\phi$$
$$=\frac{d}{dt}\left\{\frac{x_o}{\sin\phi}\right\}\cos\phi-x_o\dot{\phi} \qquad (43)$$

When the robot turns, the initial point of the robot may be invariable in time($x_o=constant$)' from the assumption. Then, we can derive a simple equation and the relation between welding speed and angular velocity of the robot :

$$\dot{\phi}=-\frac{\sin\phi^2\, v_{weld}}{x_o} \qquad (44)$$

Then, we may choose the following output equation :

$$y_p=h_p(x)=\dot{\phi} \qquad (45)$$

The error for angular velocity is defined by :

$$e_a=-\frac{\sin\phi^2 v_{weld}}{x_o}-\dot{\phi} \qquad (46)$$

Using the above equation, when the mobile robot is turning at the lattice space, the control input for two wheels of the mobile robot can be given by :

$$u_p=(K_{Pp}e_a+K_{Dp}\dot{e}_a)\begin{bmatrix}-1\\1\end{bmatrix} \qquad (47)$$

Figure 4 describes the feedback loop control algorithm incorporating the 3 cases of the robot control. The straight locomotion and the turning locomotion are controlled case by case, but torch slider control works well always. In the figure, x^d is the reference value for each controller, and e is the error value for each output.

4. Simulation Results

We consider a trajectory consisted of a straight line and curved line. In simulation, it is assumed that disturbance and noise do not affect the system. The numerical values of the system parameters used in the simulations are given in Table 1.

We considered a straight line path, $x=255\,mm$, as shown in Fig. 5(a) to give reality of the welding at the lattice space. The initial position of the robot is $(x_c,\ y_c)=(257mm,\ 0mm)$, the heading angle is $\phi=80°$. And, we assumed that the length of torch slider is initialized always $x_{ts}=175mm$. Then, the initial distance of the seam tracking sensor becomes $x_s=\left\{\frac{257}{\cos(10°)}-x_{ts}\right\}=85.964mm$. Usually, to obtain a good welding bead, the welding speed is chosen as about $7.5mm/s$ in the case of using an arc welder. Thus, we take the above stated speed for the reference welding speed. In part of turning locomotion control, we already assumed that the mobile robot is turning around one point. Thus, the forward velocity of the mobile platform is set to be zero. As the reference welding speed is $v_{weld}=7.5mm/s$ and the turning position is $x=255mm$, we can calculate the reference angular velocity of the mobile robot as shown in Fig. 6 (b). The initial length of the torch slider is $x_{ts}=175mm$. And, the PID gains were determined by repeated simulation results. The initial values of the mobile robot for simulations are shown in Table 2.

The simulation results for straight locomotion and turning locomotion are shown in Figs. 5-6. The operation of the mobile robot can be stated as follows : first, the mobile robot will track the start welding position and next, the welding process begins. In Fig. 5(a), the mobile robot tracks its start welding position in 5 seconds. There is no welding process when the robot is tracking its start welding position. Thus, the welding speed is no meaning at this time that is setting the initial welding process. After about 5 seconds, the mobile robot starts to weld, tracks well the welding line and the welding speed is kept constantly for the reference velocity. Also, the control of the seam tracking sensor is well done as shown in

Table 2 Condition values for simulations

	Straight locomotion	Turning locomotion
· *Initial* (x_c, y_c)	$(x_c, y_c)=(257mm, 0mm)$	$(x_c, y_c)=(255mm, 0mm)$
· *Initial* v_c	$v_c=0mm/s$	$v_c=0mm/s$
· *Initial* ϕ	$\phi=80°$	$\phi=80°$
· *Initial* x_{ts}	$x_{ts}=175mm$	$x_{ts}=175mm$
· *Initial* x_s	$x_s=85.964mm$	$x_s=80mm$
· *Output equation*	$h_s(x)=x_s$, $h_{p1}(q)=(x_c-255)$, $h_{p2}(\eta)=\frac{r_w}{2}(\eta_1+\eta_2)$	$h_s(x)=x_s$, $h_p(x)=\dot{\phi}$
· *Reference input*	$x_s^d=80$, $v_1^d=0$, $v_2^d=7.5$	$x_s^d=80$, $\dot{\phi}^d=-\frac{7.5\sin\phi^2}{255}$
· *Gain for the robot (Feedback gains)*	$K_{Pp}=2.5$, $K_{Ds}=2.95$	$K_{Pp}=10$, $K_{Ds}=100$
· *Gain for the torch slider (PID gains)*	$K_{Ps}=1700$, $K_{Is}=0.1$, $K_{Ds}=690$	$K_{Ps}=1700$, $K_{Is}=0.1$, $K_{Ds}=690$
· *Sampling time*	$\Delta T=0.01s$	$\Delta T=0.01s$

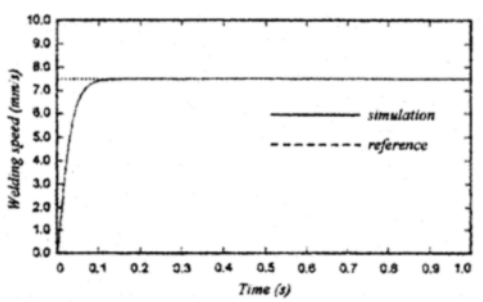

(a) The welding speed v_{weld}

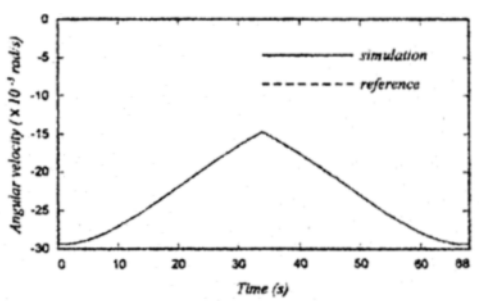

(b) The angular velocity $\dot{\phi}$

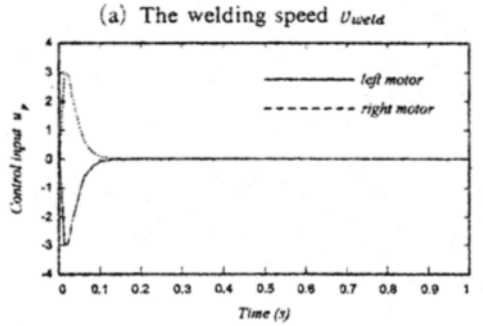

(c) Control input for mobile robot u_p

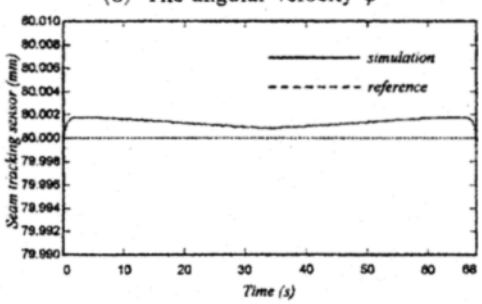

(d) Distance of the seam tracking sensor x_s

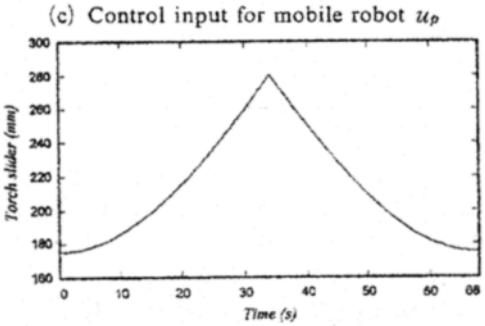

(e) Distance of the torch slider x_{ts}

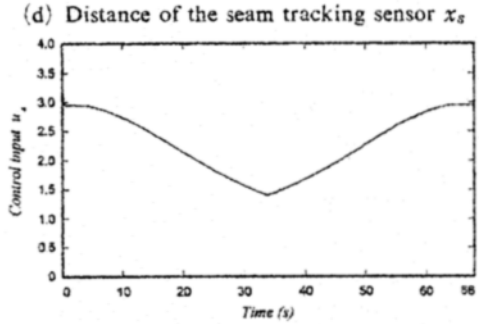

(f) Control input for torch slider u_s

Fig. 6 Simulation results of turning locomotion

Fig. 5. In simulation results for turning locomotion, there is a little error for the seam tracking sensor as shown in Fig. 6(d), but it is no affected for welding at the corner because the maximum error is about $0.002mm$. In Fig. 6(a), the mobile robot tracks well the reference angular velocity and the welding speed is kept constantly for the reference velocity.

5. Conclusion

This paper introduced a motion control method of the mobile robot for the lattice type of welding line, and proved the possibility that the mobile robot can weld the lattice type welding line. We have proposed the separated control algorithms for straight locomotion, seam tracking and turning motion. The straight locomotion control system design is done by using the dynamic nonlinear state feedback and the nonlinear state transformation which decouple the dynamic equations of the mobile platform. The PID controller method is employed for seam tracking. In addition, we have designed a turning motion controller by using the relating equation between angular velocity of the robot and given welding speed. Simulations have been done in two cases: the mobile robot welds along straight line and curved line. Through the simulation results, it can be said that the welding speed depends on initial position and initial heading angle of the mobile robot. Moreover, each gain value affects tracking time of position and welding speed. The results have proved that this system has enough ability to weld the lattice type welding line when the mobile robot is equipped for the division of the shipbuilding industry that needs the lattice type welding line. It is alone expected that these results can be effectively used to control a real system for future works.

Acknowledgement

This paper is a part of a study titled "Development of Mobile Robot for Lattice Type Welding by Using Arc-sensor" which is studied by Ministry of Commerce, Industry, and Energy support. We gratefully acknowledge the contributions and suggestions of related persons.

References

Campion, G., Bastine, G., and dAndrea-Novel, B., 1996, "Structural Properties and Classification of Kinematic and Dynamic Models of Wheeled Mobile Robots," *IEEE Transactions on Robotics and Automation*, Vol. 12, No. 1, pp. 47~62.

Chung, J. H. and Velinsky, S. A., 1999, "Robust Control of a Mobile Manipulator Dynamic Modeling Approach," *Proceedings of the 1999 American Control Conference*, pp. 2435~2439.

dAndrea-Novel, B., Bastine, G., and Campion, G., 1991, "Modelling and Control of Nonholonomic Wheeled Mobile Robots," *Proceedings of the 1991 IEEE International Conference on Robotics and Automation*, pp. 1130~1135.

Fierro, R. and Lewis, F. L., 1995, "Control of a Nonholonomic Mobile Robot: Backstepping Kinematics into Dynamics," *Proceedings of the 34th Conference on Decision & Control*, pp. 3805~3810.

Kang, C. J., Jeon, Y. B., Kam, B. O., and Kim, S. B., 2000, "Development of Continuous/Intermittent Welding Mobile Robot," *Proceedings of the National Meeting of Autumn, The Korean Welding Society*, Vol. 36, pp. 31~33.

Sarkar, N., Yun, X. and Kumar, V., 1994, "Control of Mechanical Systems With Rolling Constraints: Application to Dynamic Control of Mobile Robots," *The International Journal of Robotics Research*, Vol. 13, No. 1, pp. 55~69.

Sastry Shankar, 1999, *Nonlinear Systems Analysis, Stability, and Control*, Springer-Verlag, New York, pp. 384~448.

Yamamoto, Y. and Yun, X., 1999, "Unified Analysis on Mobility and Manipulability of Mobile Manipulators," *Proceedings of the 1999 IEEE International Conference on Robotics and Automation*, Vol 2, pp. 1200~1206.

Yamamoto, Y. and Yun, X., 1994, "Coordinating Locomotion and Manipulation of a Mobile Manipulator," *IEEE Transactions on*

Automatic Control, Vol. 39, No. 6, pp. 1326 ~1332.

Yun, X. and Yamamoto, Y., 1993, "Internal Dynamics of a Wheeled Mobile Robot," *Proceedings of the 1993 IEEE/RSJ International Conference on Intelligent Robots and Systems*, pp. 1288~1294.